

Molecular Line Observations and Chemical Modelling of Edge Cloud 2

Paul Ruffle¹, Tom Millar², Helen Roberts², Don Lubowich³, Christian Henkel⁴

ABSTRACT

Edge Cloud 2 (EC2) is a large molecular cloud with one of the largest galactocentric distances known to exist in the Milky Way. We present observations of the cloud and use these to determine its physical characteristics. We calculate a gas temperature of 20 K and a density of $n(\text{H}_2) \sim 10^4 \text{ cm}^{-3}$. Based on our CO maps, we estimate the mass of EC2 at around $10^4 M_\odot$ and continuum observations suggest a dust-to-gas mass ratio as low as 0.001. Chemical models have been developed to reproduce the abundances in EC2 and they indicate that: heavy element abundances may be reduced by a factor of five relative to the solar neighbourhood (similar to dwarf irregular galaxies and damped Lyman alpha systems); very low extinction ($A_V < 4 \text{ mag}$) due to a very low dust-to-gas ratio; an enhanced cosmic ray ionisation rate; and a higher UV field compared to local interstellar values. The reduced abundances may be attributed to the low level of star formation in this region and are probably also related to the continuing infall of low metallicity halo gas since the Milky Way formed. Finally, we note that shocks from the old supernova remnant GSH 138–01–94 may have determined the morphology and dynamics of EC2.

Subject headings: astrochemistry – dust, extinction – ISM: clouds – ISM: individual (Edge Cloud 2) – ISM: molecules – radio lines: ISM

¹National Radio Astronomy Observatory, Green Bank, WV, USA; pruffle@nrao.edu.

²School of Mathematics and Physics, The Queen’s University, Belfast, UK.

³Department of Physics and Astronomy, Hofstra University, Hempstead, NY, USA.

⁴Max-Planck-Institut für Radioastronomie, Bonn, Germany.

1. Overview

Observations of CO emission at large galactocentric distances have detected a number of molecular clouds, including Edge Cloud 2 (EC2), with an estimated kinematic galactocentric distance of $R_{\text{gc}} \sim 28$ kpc (Digel et al. 1994). EC2 appears to be up to 6 kpc further away than the next most distant cloud, and much further than the extent of the optical disk of the Milky Way, ~ 15 – 19 kpc (Fich et al. 1989; Robin et al. 1992). This is almost as far as the most distant H I detected at ~ 30 kpc (Kulkarni et al. 1982). More recently the spiral structure in the southern half of the Galaxy has been traced out to at least 25 kpc (Levine et al. 2006). EC2 has an effective radius of 20 pc and is situated 360 pc below the distant warped Galactic plane (Digel et al. 1996b). The CO luminosity of EC2 is at least a factor of 2 larger than those of the other 10 edge clouds, and is comparable to that of the Taurus Giant Molecular Cloud (Digel et al. 1994). EC2 is also the only edge cloud detected in the high-density tracer CS (Digel et al. 1996a), with CO maps showing that it has sub-structure.

EC2 was also found to have an associated H II region excited by an early B star (MR1), that appears to have triggered star formation (de Geus et al. 1993). Studies of metallicity as a function of galactocentric distance have shown that there is a galactic gradient. Spectra of MR1 (Smartt et al. 1996) indicate significant metal depletion, with elemental abundances reduced on average by some 0.5 dex. Subsequently, metal depletions of about five for C, N, and O have been calculated (Rolleston et al. 2000). NIR observations have been used to argue that MR1 has triggered the formation of young stellar objects in EC2 (Kobayashi & Tokunaga 2000), and it is thought to be the most distant cloud in the Milky Way with evidence for massive star formation (Snell et al. 2002). More recently, two embedded young star clusters have been associated with EC2, with 72 and 66 members respectively identified as T Tauri associations (Yasui et al. 2006, 2007). EC2 is also associated with the approaching side of the H I shell from supernova remnant (SNR) GSH 138–01–94 (Stil & Irwin 2001), setting the distance $R_{\text{gc}} \sim 24$ kpc for EC2.

2. Observations

We have searched for emission from a number of molecules towards EC2 in order to constrain its physical conditions and chemical composition (Ruffle et al. 2007). Such molecular evolution in low metallicity Galactic clouds provides a local laboratory in understanding molecular gas in extragalactic sources such as high- z quasars. We detected continuum emission and a large number of molecular transitions in EC2, completing over 210 hours of observations using the JCMT 15 m, ARO 12 m, Effelsberg 100 m and IRAM 30 m telescopes. CO maps were also made, and used to calculate deconvolved line intensities. Fig. 1 shows ex-

amples of our molecular line detections, and Fig. 2 shows CO 2–1 intensity contours overlaid on 1.2 mm dust map, showing the correspondence of peak CO and dust emission.

3. Analysis

A temperature of 20 K was estimated from our hyperfine detections of ammonia and a gas density of $n(\text{H}_2) \sim 10^4 \text{ cm}^{-3}$ was determined by comparing LVG models of a number of species to their deconvolved line detections. Molecular abundances were also determined from the LVG models and found to be in good agreement with abundances calculated directly from the deconvolved line intensities. Taking the clumpy structure of EC2 into account, we also calculated $M_{\text{EC2}} \sim 10^4 M_{\odot}$, and from the peak continuum emission we calculated a dust mass for EC2 and a dust-to-gas mass ratio ≥ 0.001 .

4. Chemical Modelling

To establish the most likely chemical and physical properties of EC2 and to see whether it is typical of material which has been less processed, we made a pseudo-time-dependent chemical kinetic model. This uses our observationally derived temperatures and densities and varies elemental initial abundances (IA), photon flux (UV), cosmic ray ionisation (CRI) rate and gas-to-dust ratio (A_V), in an attempt to fit the observed results. For example, Fig. 3 plots the agreement factor for models with varying A_V and an increasing UV field. We found that heavy elements may be depleted by about a factor of five relative to local molecular clouds. The models also suggest a high UV photon field in EC2 ($10\text{--}20 \times$ local values), where an increased UV field allows for values of A_V up to 4 mag, especially if this increased field is combined with an increase in CRI ($10\text{--}20$ times the standard interstellar rate of $1.3 \times 10^{-17} \text{ s}^{-1}$). Gas densities much above $n(\text{H}_2) = 1.2 \times 10^4 \text{ cm}^{-3}$ are excluded by the models, even if the UV field is increased. Some of our models indicate that steady-state is reached very quickly after around 5,000 years (Fig. 4) and that a high UV field can reduce this time to just ~ 500 yr.

5. Conclusions

Table 1 compares molecular abundances ratios in EC2 relative to HCO^+ with L134N (Dickens et al. 2000) and TMC-1 (Pratap et al. 1997), and relative to H_2 with translucent clouds (Turner 2000). In the context of ratios relative to HCO^+ , sulfur-bearing molecules

appear to be very over-abundant by at least an order of magnitude compared to local dark clouds. The observed high abundances of the radicals C_2H and CN are typical of photon-dominated regions (PDRs). This may be related to a large value of the UV flux to grain surface area when compared to local clouds. In particular, we found that our best-fit models are consistent with reduced elemental abundances and a low dust-to-gas mass ratio. Such reduced abundances may be attributed to the low level of star formation in this region, and are probably also related to the continuing infall of low metallicity halo gas since the Milky Way formed. In addition, although EC2 does contain young stars, there is no evidence of the late-type stars which produce dust grains, thereby justifying the assumption of a high ratio of UV flux to grain surface area. We conclude therefore, that despite the position of EC2 in the Galaxy, UV photons (rather than cosmic rays) play an important role in establishing its detailed chemical composition.

Given that EC2 is in a region of extremely low gas pressure and very small spiral arm perturbation, the question remains as to the origin of the structure and chemistry in EC2. It has been shown that the SNR associated with EC2, GSH 138–01–94, is the largest and oldest SNR known to exist in the Milky Way (Stil & Irwin 2001). It consists of a H I shell with an expansion velocity of $\sim 12 \text{ km s}^{-1}$, an expansion age of 4.3 Myr and a timescale for dissolving into the ISM of 18 Myr. EC2 could, therefore, be as young as the ages derived from our time-dependent calculations. We conclude that the formation, structure and subsequent chemistry of EC2 may be the direct result of shock fronts from GSH 138–01–94 propagating through the medium sometime between 1,000 and 10,000 years ago. The role of the SNR is reinforced by the three-dimensional geometry of GSH 138–01–94, EC2 and the embedded star cluster, as well as the cluster’s age ($\sim 1 \text{ Myr}$, much less than the SNR’s expansion age of 4.3 Myr), strongly suggesting that the star formation observed in EC2 was triggered by the SNR H I shell (Yasui et al. 2006).

6. Summary of EC2 properties

Position A $\alpha_{2000} = 02^{\text{h}} 48^{\text{m}} 38.5^{\text{s}}$ $\delta_{2000} = 58^{\circ} 28' 28.1''$.

Radial Velocity $v_{\text{rad}} = -103.7 \text{ km s}^{-1}$.

Temperature $T = 20 \text{ K}$.

Density $n(\text{H}_2) \sim 10^4 \text{ cm}^{-3}$.

Cosmic Ray Ionisation $10\text{--}20 \times 1.3 \times 10^{-17} \text{ s}^{-1}$.

UV Photon Field $10\text{--}20 \times \text{local ISM values}$.

Initial Abundance 20 per cent of local ISM values.

Extinction $A_V < 4$ mag.

Dust to Gas Ratio $M_{\text{dust}}/M_{\text{gas}} = 0.001\text{--}0.015$.

Mass $M_{\text{EC2}} \approx 10^4 M_{\odot}$.

REFERENCES

- de Geus, E. J., Vogel, S. N., Digel, S. W., & Gruendl, R. A. 1993, *ApJ*, 413, L97
- Dickens, J. E., Irvine, W. M., Snell, R. L., et al. 2000, *ApJ*, 542, 870
- Digel, S., de Geus, E., & Thaddeus, P. 1994, *ApJ*, 422, 92
- Digel, S. W., de Geus, E. J., Henkel, C., Hüttemeister, S., & Thaddeus, P. 1996a, in *IAU Symp. 170: CO: Twenty-Five Years of Millimeter-Wave Spectroscopy*, 20P
- Digel, S. W., Hunter, S. D., Mukherjee, R., et al. 1996b, in *IAU Symp. 170: CO: 25 Years of mm-Wave Spectroscopy*, 22
- Fich, M., Blitz, L., & Stark, A. A. 1989, *ApJ*, 342, 272
- Kobayashi, N. & Tokunaga, A. T. 2000, *ApJ*, 532, 423
- Kulkarni, S. R., Heiles, C., & Blitz, L. 1982, *ApJ*, 259, L63
- Levine, E. S., Blitz, L., & Heiles, C. 2006, *Science*, 312, 1773
- Pratap, P., Dickens, J. E., Snell, R. L., et al. 1997, *ApJ*, 486, 862
- Robin, A. C., Creze, M., & Mohan, V. 1992, *ApJ*, 400, L25
- Rolleston, W. R. J., Smartt, S. J., Dufton, P. L., & Ryans, R. S. I. 2000, *A&A*, 363, 537
- Ruffle, P. M. E., Millar, T. J., Roberts, H., et al. 2007, *ApJ*, 671, 1766
- Smartt, S. J., Dufton, P. L., & Rolleston, W. R. J. 1996, *A&A*, 305, 164
- Snell, R. L., Carpenter, J. M., & Heyer, M. H. 2002, *ApJ*, 578, 229
- Stil, J. M. & Irwin, J. A. 2001, *ApJ*, 563, 816
- Turner, B. E. 2000, *ApJ*, 542, 837

Yasui, C., Kobayashi, N., Tokunaga, A. T., Terada, H., & Saito, M. 2006, *ApJ*, 649, 753

Yasui, C., Kobayashi, N., Tokunaga, A. T., Terada, H., & Saito, M. 2007, *ArXiv e-prints*,
711

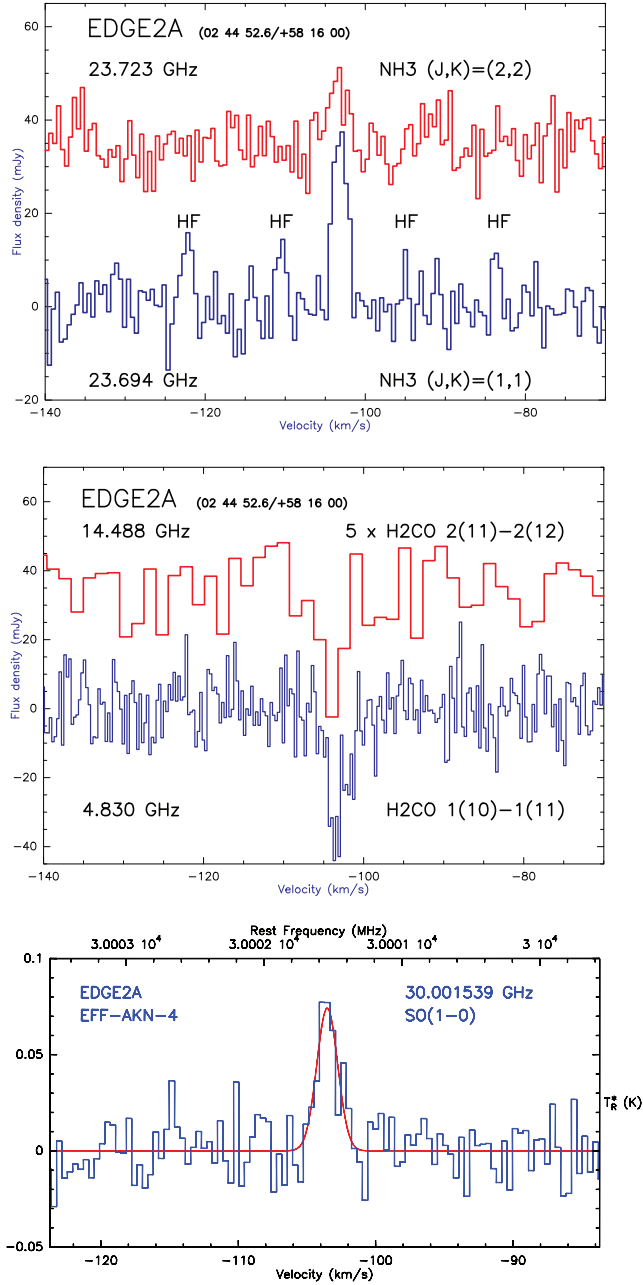


Fig. 1.— EC2 spectra observed at the MPIfR Effelsberg 100 m position A: (top) NH₃ (J,K) = (1,1) and (2,2) (HF = group of satellite hyperfine components). (middle) H₂CO 2_{1,1}–2_{1,2} and 1_{1,0}–1_{1,1}. Note that the scale for the 2_{1,1}–2_{1,2} transition has been multiplied by 5. (bottom) SO 1₀–0₁.

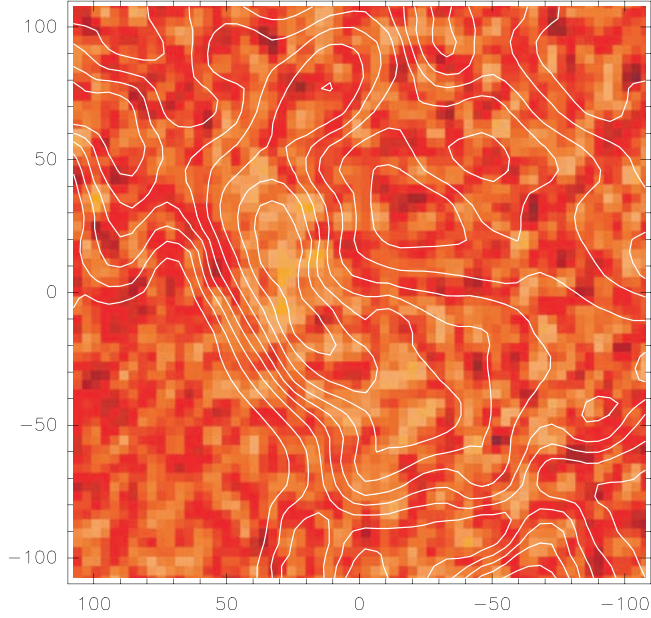


Fig. 2.— CO 2–1 intensity contours (JCMT 15 m) overlaid on 1.2 mm dust map (IRAM 30 m), showing the correspondence of peak CO and dust emission. Contour levels 10% of peak, dashed 50% (*fwhp*). CO peak $T_{\text{R}}^* = 7.124$ K, rms = 0.22 K. Dust peak 20.3 mJy/beam ($\theta_{\text{b}} = 11''$), rms = 6.35 mJy/beam. Axis offsets in arcsec.

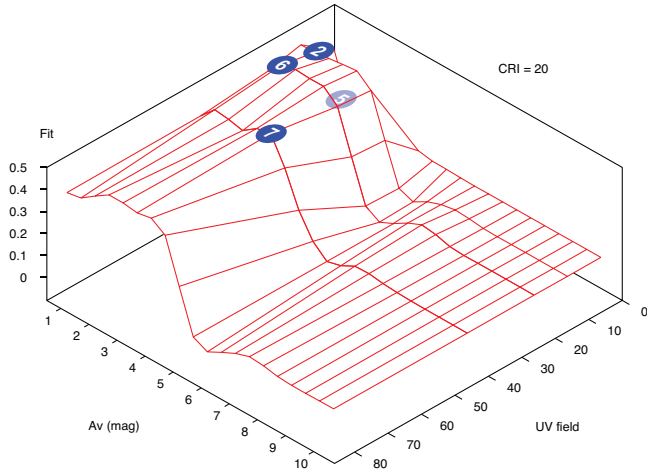


Fig. 3.— Agreement factor for chemical models with varying A_{V} and an increasing UV field, with $T = 20$ K; $n(\text{H}_2) = 1.2 \times 10^4 \text{ cm}^{-3}$; CRI rate = $20 \times$ the standard ISM rate of $1.3 \times 10^{-17} \text{ s}^{-1}$; and most initial abundances reduced by a factor of 5 from typical local ISM values. Numbered disks indicate specific models relative to the parameter surface, with Model 2 being our best fit.

Table 1. Comparison of molecular abundances ratios relative to HCO^+ and H_2 in EC2 (position A), L134N (center), TMC-1 (average) and L134N (range) (Dickens et al. 2000; Pratap et al. 1997), Trans(lucent) cloud observations by (Turner 2000). For EC2 $T_{\text{ex}} = 20$ K, $n(\text{H}_2) = 1.2 \times 10^4 \text{ cm}^{-3}$ and $N(\text{H}_2) = 7.4 \times 10^{22} \text{ cm}^{-2}$ assumed in calculation of fractional abundances.

Molecule		X/ HCO^+	L134N	TMC-1	L134N range	Trans	X/ H_2
CO	1-0	17078	11000 ^b	7800 ^b			3.3×10^{-07}
¹³ CO	1-0	2919	172 ^a	122 ^a	111-188		5.7×10^{-08}
C ¹⁸ O	1-0	214	22.00	15.60	14.2-24		4.2×10^{-09}
C ¹⁷ O	1-0	<38.8	—	—			$<7.6 \times 10^{-10}$
CO	2-1	6070	11000 ^b	7800 ^b			1.2×10^{-07}
¹³ CO	2-1	1308	172 ^a	122 ^a			2.6×10^{-08}
C ¹⁸ O	2-1	92	22.00	15.60			1.8×10^{-09}
CO	3-2	3389	11000 ^b	7800 ^b			6.6×10^{-08}
¹³ CO	3-2	439	172 ^a	122 ^a			8.6×10^{-09}
C ¹⁸ O	3-2	<27.2	22.00	15.60			$<5.3 \times 10^{-10}$
Cl		53020	—	—			1.0×10^{-06}
CS	2-1	2.33	0.124	0.320	0.069-0.138	1.1×10^{-08}	4.6×10^{-11}
CS	3-2	0.26	0.124	0.320			5.1×10^{-12}
C ³⁴ S	3-2	<0.08	—	—			$<1.5 \times 10^{-12}$
CN ^d		1.58	0.061	0.070	<0.045-0.069		3.1×10^{-11}
SO	1-0	13.0	0.719	0.130	0.264-0.738	3.2×10^{-08}	2.5×10^{-10}
SO	3-2	2.87	0.719	0.130	0.264-0.738		5.6×10^{-11}
DCO ⁺	1-0	<0.08	—	—			$<1.6 \times 10^{-12}$
H ¹³ CO ⁺	1-0	<0.06	c	c			$<1.1 \times 10^{-12}$
HCO ⁺	1-0					2×10^{-09}	2.0×10^{-11}
DCN	1-0	<1.13					$<2.2 \times 10^{-11}$
H ¹³ CN	1-0	<0.07	c	c			$<1.4 \times 10^{-12}$
HCN	1-0	0.76	0.925	0.490	0.555-0.968	3.6×10^{-08}	1.5×10^{-11}
HNC	1-0	0.24	3.251	1.680	1.324-3.963	2.5×10^{-09}	4.7×10^{-12}
C ₂ H ^e	1-0	35.5	0.288	0.300	0.171-0.333	6.6×10^{-08}	7.0×10^{-10}
N ₂ H ⁺	1-0	<0.07	0.077	0.013	0.031-0.077	$\sim 1 \times 10^{-09}$	$<1.3 \times 10^{-12}$
H ₂ CO		3.87				6.3×10^{-09}	7.6×10^{-11}
NH ₃		4.0	7.635	2.770	4.284-9.127	2.1×10^{-08}	7.8×10^{-11}
HC ₃ N	9-8	<0.18	0.054	0.150	0.030-0.073	5×10^{-10}	$<3.5 \times 10^{-12}$
CH ₃ OH	2-1		0.641	0.099	0.311-0.641	1.8×10^{-08}	

^aA ¹³CO/C¹⁸O ratio of 7.81 was assumed in L134N and TMC-1.

^bA ¹²CO/C¹⁸O ratio of 500 was assumed in L134N and TMC-1.

^cA ¹²C/¹³C ratio of 64 was assumed in L134N and TMC-1.

^dFrom the sum of the two 113.49 GHz components assuming a relative intensity of 0.456.

^eFrom the 87.317 GHz component assuming a relative intensity for this line of 0.4167.

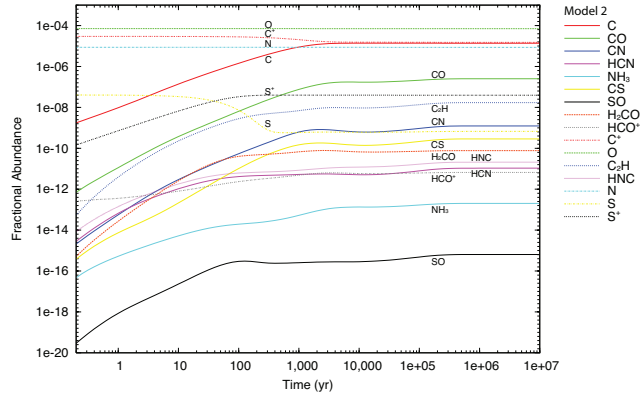


Fig. 4.— Fractional abundances varying over time for Model 2, where $A_V = 1$ mag, $\text{CRI} = 20 \times 1.3 \times 10^{-17} \text{ s}^{-1}$, $\text{UV} = 1 \times \text{local ISM values}$, $\text{IA} = 0.2 \times \text{local ISM values}$, $n(\text{H}_2) = 1.2 \times 10^4 \text{ cm}^{-3}$ and $T = 20 \text{ K}$.